Theoretical-experimental Modeling of Bolted Joint Interface in Milling of Grey Cast Iron HT250

Hongliang Tian, Dalin Zhu, Hongling Qin

***Abstract*—The concept of virtual material was presented for the first time when the flexible joint interface may be viewed as a virtual material with the same cross area. The virtual material is rigidly connected with two components situated in both sides of flexible joint interface. Introducing an element, a complex assembled part including a joint interface could be equaled as a simple component without any joint interface so as to simplify the complicated problem about flexible joint interface. The interaction between normal and tangential characteristics of fixed interface considered, a lot of exact analytical expressions of elastic modulus, shear modulus, Poisson ratio and density were deduced from virtual material according to Hertz contact theory and fractal theory. Adopting experimental results about a series of test specimens, the exact analytic solutions for virtual material's parameters were verified in terms of qualitative comparison principle of resembling vibration shapes and quantitative comparison principle of the natural frequencies. The virtual material model vibration shapes show good agreement with the experimental results. The relative errors between the virtual material model natural frequencies and the experimental ones are between -9% and 5%.**

***Index Terms*—bolted joint interface, fractal theory, Hertz contact theory, natural frequency, vibration shape, virtual material.**

I. Introduction

If we now assemble single members into a built-up structure, prediction of the structure's behavior can be quite involved, even though the behavior of a single member is well known. Information about the details of coupling between members and the contact behavior is still needed. Chlebus and Dybala [1] described a method of calculation of the static properties of guideway joints using finite element analysis. In its computational models, the presented method considered phenomena occurring in the contact layer of these joints. Iwan [2-4] presented a model for the hysteretic behavior of materials and structures, based on an approach which viewed the system as consisting of a series of ideal elastoplastic elements. The effect of the roundedness of the hysteresis loop on the nature of the response was investigated. In experiment, of particular interest is the work of [5], where using stiffness influential factors, the theoretical modal shape is compared with the experimental one all around to validate the identification approach. Allowing prediction of frequency-response functions at the tool tip by receptance coupling of tools and holders to the spindle, Namazi et al. [6] identified the springs by minimizing the error between the experimentally measured and estimated frequency response of the spindle assembly. Brehm et al. [7] presented a numerical benchmark study and an experimental case study, where the suggested approach leaded to satisfying results with limited additional numerical effort while the application of the modal assurance criterion (MAC) fails to find the correct mode shapes. Becker et al. [8] exercised an algorithm on a tool/toolholder interface, with highly repeatable results for stiffness determination. The concept of zero thickness elements was discussed in detail in Mayer and Gaul [9]. A typical zero thickness element is depicted in Fig. 1. A zero thickness element consists of two four-node quadrilateral elements which face each other. In contact mechanics, we are interested in the relative displacement field of the contacting surfaces. This is expressed for zero thickness elements through the relative displacement between the top and the bottom quadrilateral.

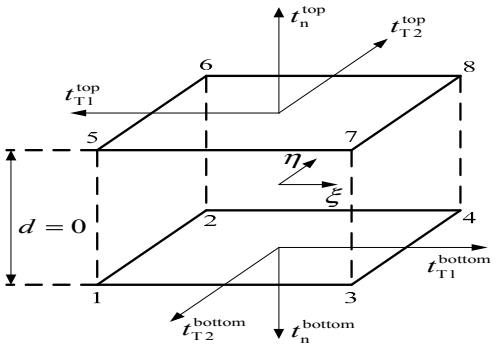

Figure 1. Zero thickness element of joint interface.

The concept of virtual material was developed when the flexible joint interface could be considered a virtual material with the same cross area. The virtual material is rigidly connected with two components situated in both sides of flexible joint interface. By adding an element, a complex assembled part including a joint interface could be equaled as a simple component without a joint interface in order to simplify the complicated problem about flexible joint interface.

II. Exact Solutions for Bolted Joint Interface Virtual Material's Parameters

A complicated assembled part including a flexible joint interface is shown in Fig. 2. The complication is brought about by the relative displacement between component 1 and 2.

Manuscript received February 28, 2011

College of Mechanical and Material Engineering, China Three Gorges University, 443002, Yichang city Hubei province, the People's Republic of China(e-mail: thl19732003@yahoo.com.cn).

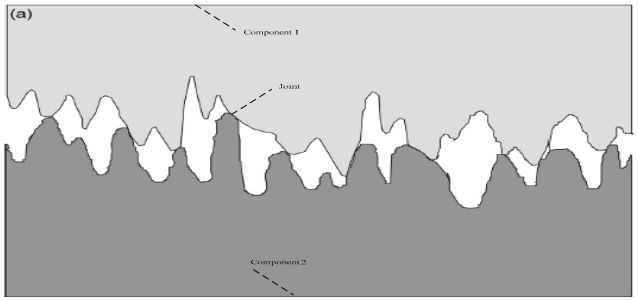

Figure 2. A complicated assembled part including a flexible joint interface.

Now, the flexible joint interface may be considered a virtual material with the same cross area. A lot of analytic solutions of elastic modulus, Poisson ratio, density and thickness could be attained for such virtual material using theoretical method. The virtual material is rigidly connected with component 1 and 2 situated in both sides of flexible joint interface. Thereby by adding an element, a complicated assembled part including a joint interface in Fig. 2 could be equaled as a simple component without a joint interface so as to simplify the complicated problem about flexible joint interface. A simple component including a virtual material is shown in Fig. 3. The simple component has 3 material properties, whose physical properties suddenly change at the virtual material.

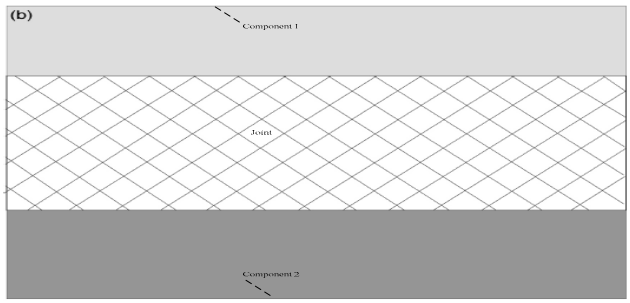

Figure 3. A simple component including a virtual material.

In terms of Hertz contact theory [10] and fractal theory [11], the elastic modulus, Poisson ratio, and density of fixed machined joint interface virtual material are provided directly without details of derivation for the sake of brevity of the paper as below, respectively

$$E = \frac{2D}{3\pi^2} E' G^{1-D} a_{\mathrm{L}}^{0.5D} (a_{\mathrm{c}}^{-0.5} - a_{\mathrm{L}}^{-0.5}) \quad \text{if } A_{\mathrm{r}} > A_{\mathrm{rc}} \tag{1}$$

$$\upsilon = \frac{(1+\mu')E^*}{G_x^*} - 1 \tag{2}$$

$$\rho = \frac{\rho_1 h_1 + \rho_2 h_2}{h} = \frac{\rho_1 h_1 + \rho_2 h_2}{h_1 + h_2} \tag{3}$$

in which D is fractal dimension of a surface profile, E' the equivalent elastic modulus of two contacting surfaces, G fractal roughness parameter, a_{L} the area of the largest elastic microcontact, a_{c} the critical area demarcating the elastic and plastic regimes, A_{r} the real area of the contact region, and A_{rc} the real critical contact area, μ' the equivalent Poisson ratio of two contact rough surfaces, E^* the dimensionless elastic modulus of bolted joint interface virtual material, G_x^* the dimensionless shear modulus of virtual material, ρ_1 and ρ_2 the densities of the surfaces 1 and 2, and h_1 and h_2 the normal heights of surfaces 1 and 2, respectively.

$$\frac{1}{E'} = \frac{1-\mu_1^2}{E_1} + \frac{1-\mu_2^2}{E_2} \tag{4}$$

$$a_{\mathrm{L}} = \frac{2-D}{D} A_{\mathrm{r}} \tag{5}$$

$$a_{\mathrm{c}} = \frac{G^2}{(0.5K\phi)^{\frac{2}{D-1}}} \tag{6}$$

$$A_{\mathrm{rc}} = \frac{D}{2-D} a_{\mathrm{c}} \tag{7}$$

$$\mu' = \frac{E'}{2G'} - 1 \tag{8}$$

$$E^* = \frac{E}{E'} \tag{9}$$

$$G_x^* = \frac{G_x}{G'} \tag{10}$$

where μ_1 and μ_2 denote Poisson ratios of surfaces 1 and 2, E_1 and E_2 the elastic moduli of surfaces 1 and 2, K the factor relating hardness to yield strength, ϕ the material property, G' the equivalent shear modulus of two contacting rough surfaces, G_x the shear modulus of virtual material.

$$\frac{1}{G'} = \frac{2-\mu_1}{G_1} + \frac{2-\mu_2}{G_2} \tag{11}$$

$$G_x = \frac{16}{\pi} \sqrt[3]{1 - \frac{\beta}{f}} G' \left[\left(\frac{a_{\mathrm{L}}}{a_{\mathrm{c}}} \right)^{0.5D} - 1 \right] \quad \text{if } A_{\mathrm{r}} > A_{\mathrm{rc}} \tag{12}$$

where G_1 , G_2 the shear moduli of surfaces 1 and 2, $\beta = Q_x / P$, Q_x the tangential load applied on the virtual material, P the normal load at the joint interface, f a constant coefficient of kinetic friction whose value is determined by the materials and the physical conditions of the interface.

$$P(A_{\mathrm{r}} > A_{\mathrm{rc}}) = \begin{cases} \dfrac{4\sqrt{\pi}D}{3(3-2D)} E' G^{D-1} a_{\mathrm{L}}^{0.5D} (a_{\mathrm{L}}^{1.5-D} - a_{\mathrm{c}}^{1.5-D}) + \\ \dfrac{D}{2-D} K \sigma_{\mathrm{y}} a_{\mathrm{L}}^{0.5D} a_{\mathrm{c}}^{1-0.5D} \quad \text{if } D \neq 1.5 \\ \sqrt{\pi G} E' a_{\mathrm{L}}^{0.75} \ln \dfrac{a_{\mathrm{L}}}{a_{\mathrm{c}}} + 3K \sigma_{\mathrm{y}} a_{\mathrm{L}}^{0.75} a_{\mathrm{c}}^{0.25} \quad \text{if } D = 1.5 \end{cases} \tag{13}$$

where σ_{y} represents the yield strength of the softer material.

III. Effective Verification of Bolted Joint Interface Virtual Material's Parameters

After investigating XHK5140 automatic tool-changing CNC vertical boring and milling machine tool from 847 factory Huazhong gongxue institute, a gantry beam-column specimen composed of two 700 mm × 800 mm × 50 mm hollow thin plates is designed and manufactured, which is connected by 11 M24 bolts, as shown in Fig. 4.

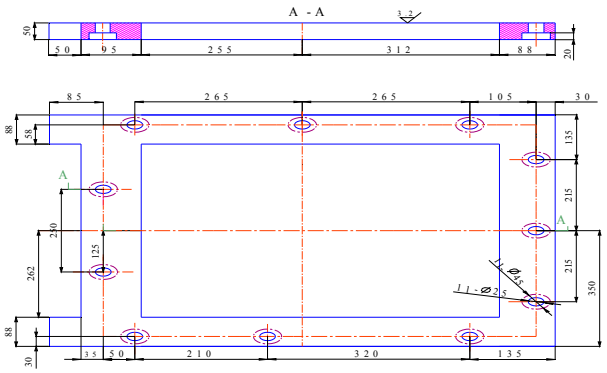

(a) Plane dimension of beam-column specimen

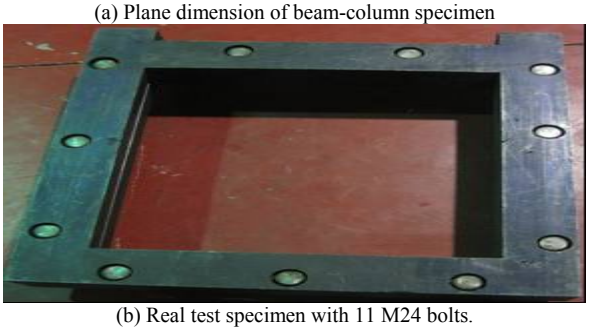

(b) Real test specimen with 11 M24 bolts.

(c) Experimental setup and test specimen freely supported.

Figure 4. Beam-column specimen including bolted joint interfaces.

The measured milling profile surface of bolted joint interfaces in Fig. 4(b) is plotted in Fig. 5 utilizing stylus profiler with type TR110.

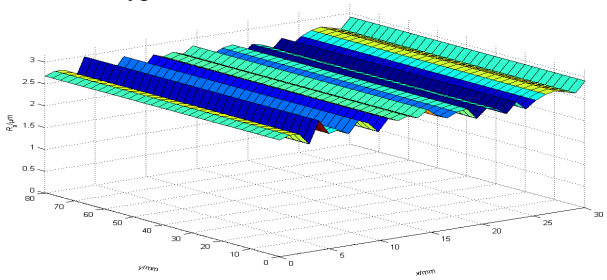

Figure 5. Measured milling surface of bolted joint interfaces.

Under the same pre-tightening torque of 45 N•m, 90 N•m and 135 N•m executing on each bolt respectively, the parameters of joint interface virtual material are listed in Table Ⅰ. Under pre-tightening torque of 135 N•m applying each bolt, some parameters of Yoshimura model [12] are $k_x = k_y = 9.16\text{e}7$ N/m, $k_z = 3.75\text{e}10$ N/m, $c_x = c_y = 6.39\text{e}5$ N•s/m and $c_z = 5.83\text{e}8$ N•s/m. The finite element models of beam-column specimen are displayed in Fig. 6.

TABLE Ⅰ. VIRTUAL MATERIAL'S PARAMETERS CORRESPONDING TO THREE CONDITIONS

T (N•m)	E (GPa)	υ	ρ (kg/m^3)
45	0.352	0.23	7340
90	0.541	0.25	7340
135	0.885	0.26	7340

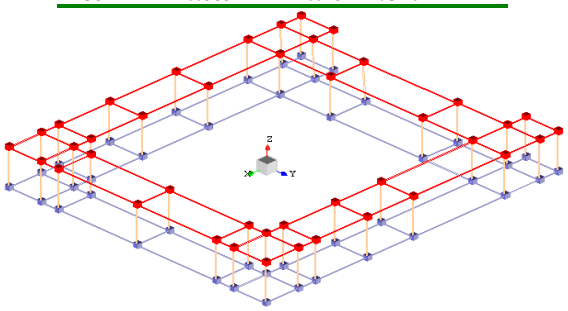

(a) Experimental model with 84 nodes.

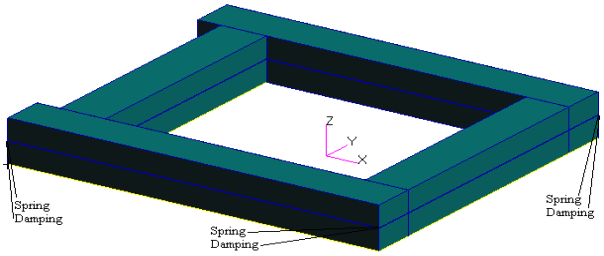

(b) Yoshimura model with 56 nodes and 28 elements.

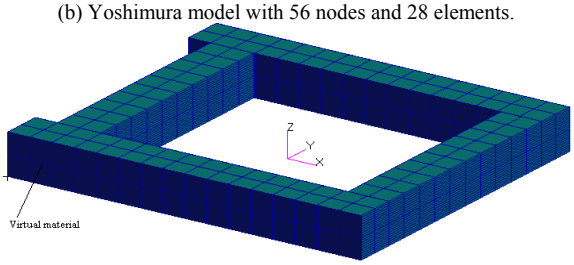

(c) Virtual material model with 3608 nodes and 2496 elements.

Figure 6. Finite element model of beam-column specimen.

When each bolt is applied by the same pre-tightening torque of 135 N•m, the frequency response of receptance and the first five-order vibration shapes of the structure are identified by a modal hammering impact testing experimental method and two theoretical models, which are illustrated in Fig. 7 and Table Ⅱ. The experimental first five-order vibration shapes are two 800 mm sides bending along +z axis and –z axis in plane zox, extending and shortening in the diagonal direction, bending along +z axis and –z axis, two 800 mm sides bending along +y axis and –y axis in plane xoy, bending along z axis, respectively. Yoshimura model vibration shapes are not all the same as the experimental ones while virtual material model vibration shapes give excellent agreement with the experimental ones. To one's regret, Yoshimura model meets an overwhelming challenge to be overcome!

The first five-order natural frequencies of the structure are identified by a modal hammering impact testing experimental method and two theoretical models, which are illustrated in Table Ⅲ. The relative errors between the virtual material model natural frequencies of the first 5 order and the experimental ones are between -9% and 5%.

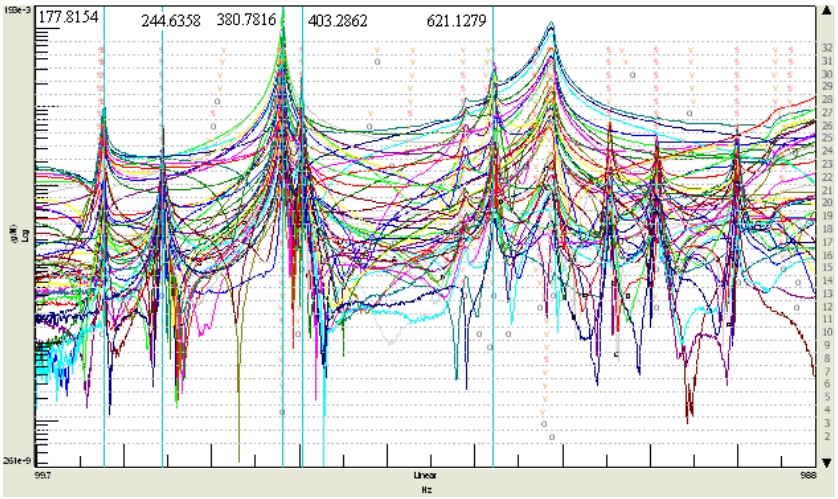

Figure 7. Curve of frequency response of receptance by experiment in 252 directions.

TABLE Ⅱ. COMPARISON OF TWO THEORETICAL VIBRATION SHAPES WITH EXPERIMENTAL ONES

Order	Experimental vibration shape	Yoshimura model vibration shape	Virtual material model vibration shape
1	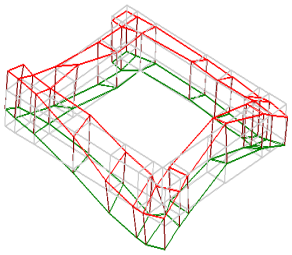	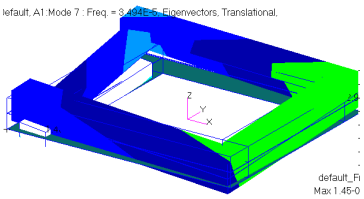	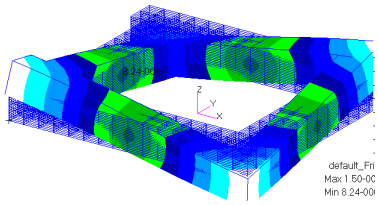
2	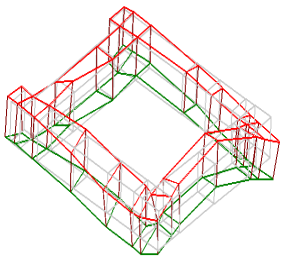	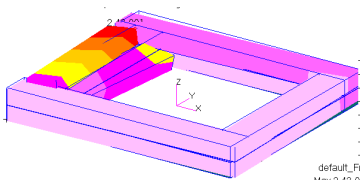	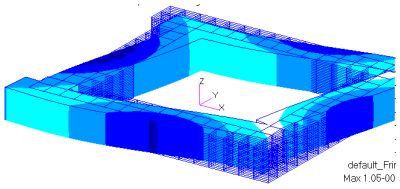
3	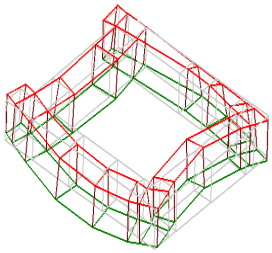	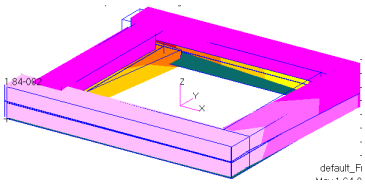	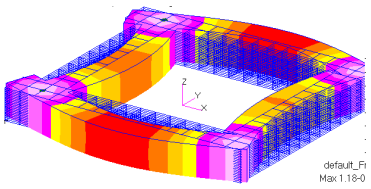
4	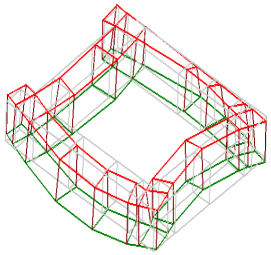	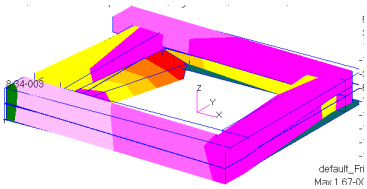	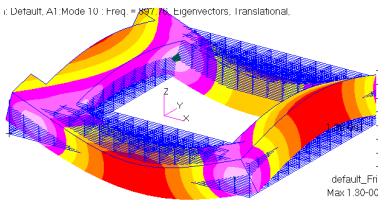
5	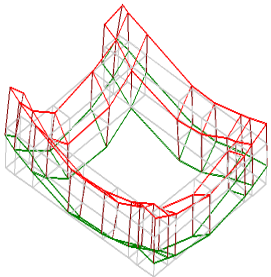	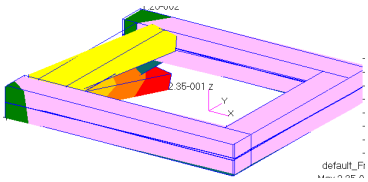	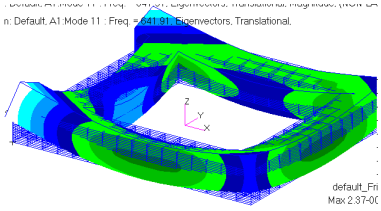

TABLE Ⅲ. COMPARISON OF TWO THEORETICAL FIRST FIVE-ORDER NATURAL FREQUENCIES WITH EXPERIMENTAL ONES

T **(N•m)**	**Natural frequency (Hz)**	f_1 **(Hz)**	f_2 **(Hz)**	f_3 **(Hz)**	f_4 **(Hz)**	f_5 **(Hz)**
45	Experimental natural frequency	164.6081	244.3881	371.0363	403.1976	597.9893
	Virtual material model natural frequency	155.36	237.16	378.71	389.64	621.41
	Virtual material model relative error (%)	-5.6183	-2.9576	2.0682	-3.3625	3.9166
90	Experimental natural frequency	172.6363	244.4485	375.7162	403.0605	611.3239
	Virtual material model natural frequency	158.57	249.38	382.63	392.52	637.52
	Virtual material model relative error (%)	-8.1479	2.0174	1.8402	-2.6151	4.2851
135	Experimental natural frequency	177.8154	244.6358	380.7816	403.2862	621.1279
	Yoshimura model natural frequency	3.494e-5	2.6043e-5	5.8284e-5	8.2391e-5	9.3616e-5
	Virtual material model natural frequency	163.66	255.44	385.45	397.76	641.91
	Yoshimura model relative error (%)	——	——	——	——	——
	Virtual material model relative error (%)	-7.9607	4.4164	1.2260	-1.3703	3.3459

IV. Conclusion

A novel dynamic modeling method of the bolted joint interfaces is put forward in this manuscript to improve the modeling accuracy. The concept of virtual material was also suggested. The interaction between normal and tangential characteristics of bolted joint interface considered, a lot of exact analytic solutions of elastic modulus, shear modulus, Poisson ratio and density were deduced via virtual material.

Using experimental results about many test specimens, the analytic solutions for virtual material's parameters were verified according to qualitative comparison principle of resembling vibration shapes and quantitative comparison principle of the natural frequencies. Theoretical vibration shapes are in good agreement with experimental results. The relative errors between the virtual material model natural frequencies and the experimental ones are between -9% and 5%.

All vibration shapes predicted by the classic Yoshimura model are not the same as the experimental ones, which is a natural shortcoming not to be overcome. The basic principle for the classic Yoshimura model is that many no-coupled spring-damping elements are applied to simulate the relative movement of the two neighboring components distributed on both sides of joint interface, so its predicting vibration shapes certainly include such three ones as *x*-axis translating, *y*-axis translating, and *z*-axis translating. Of course, the conclusion is false in the actual engineering, for example, the vibration shapes of thin plate bolted joint interface mainly take the form of bending, but not translating.

The establishment of the model in this article will provide a theoretical-experimental base for the precise dynamic modeling of bolted joint interfaces in CNC machine tools. The virtual material model is applicable to any bolted joint interfaces, but not to the movable ones.

References

[1] Edward Chlebus and Bogdan Dybala, "Modelling and Calculation of Properties of Sliding Guideways," International Journal of Machine Tools & Manufacture, 39 (12), 1999, pp. 1823-1839.

[2] W. D. Iwan, "A Distributed-Element Model for Hysteresis and Its Steady-State Dynamic Response," Journal of Applied Mechanics, 33 (4), 1966, pp. 893-900.

[3] W. D. Iwan, "On a Class of Models for the Yielding Behavior of Continuous and Composite Systems," Journal of Applied Mechanics, 34 (3), 1967, pp. 612-617.

[4] Y. Song, C. J. Hartwigsen, D. M. McFarland, A. F. Vakakis and L. A. Bergman, "Simulation of Dynamics of Beam Structures With Bolted Joints Using Adjusted Iwan Beam Elements," Journal of Sound and Vibration, 273 (1-2), 2004, pp. 249-276.

[5] Kuanmin Mao, Bin Li, Jun Wu, and Xinyu Shao, "Stiffness Influential Factors-Based Dynamic Modeling and Its Parameter Identification Method of Fixed Joints in Machine Tools," International Journal of Machine Tools & Manufacture, 50 (2), 2010, pp. 156-164.

[6] Mehdi Namazi, Yusuf Altintas, Taro Abe and Nimal Rajapakse, "Modeling and Identification of Tool Holder-Spindle Interface Dynamics," International Journal of Machine Tools & Manufacture, 47 (9), 2007, pp. 1333-1341.

[7] Maik Brehm, Volkmar Zabel and Christian Bucher, "An Automatic Mode Pairing Strategy Using an Enhanced Modal Assurance Criterion Based on Modal Strain Energies," Journal of Sound and Vibration, 329 (25), 2010, pp. 5375-5392.

[8] Patricia J. Wyatt Becker, Robert H. Wynn, Jr., Edward J. Berger and Jason R. Blough, "Using Rigid-Body Dynamics to Measure Joint Stiffness," Mechanical Systems and Signal Processing, 13 (5), 1999, pp. 789-801.

[9] M. H. Mayer and L. Gaul, "Segment-to-Segment Contact Elements for Modelling Joint Interfaces in Finite Element Analysis," Mechanical Systems and Signal Processing, 21 (2), 2007, pp. 724-734.

[10] Y. Zait, V. Zolotarevsky, Y. Kligerman and I. Etsion, "Multiple Normal Loading-Unloading Cycles of a Spherical Contact Under Stick Contact Condition," Journal of Tribology, 132 (4), 2010, pp. 041401-1-041401-7.

[11] Jeng Luen Liou and Jen Fin Lin, "A New Method Developed for Fractal Dimension and Topothesy Varying With the Mean Separation of Two Contact Surfaces," Journal of Tribology, 128 (3), 2006, pp. 515-524.

[12] M. Yoshimura, "Computer-Aided Design Improvement of Machine Tool Structure Incorporating Joint Dynamics Data," Annals of the CIRP, 28 (1), 1979, pp. 241-246.